Variational calculations of few-body nuclei

R. B. Wiringa
Physics Division, Argonne National Laboratory, Argonne, Illinois 60439
(Received 12 December 1990)

Improved variational wave functions for use in microscopic studies of few-body nuclei are presented. The trial functions are constructed from pair-correlation operators, which include central, spin, isospin, tensor, and spin-orbit components, and triplet-correlation operators, which include components induced by three-nucleon potentials. Energy expectation values are calculated using Metropolis Monte Carlo integration. Variational parameter searches are made using energy differences to reduce the effect of statistical fluctuations on the choice of optimal trial functions. Results are reported for ground-state binding energies of ^{3}H and ^{4}He using the Reid v_8 and Argonne v_{14} two-nucleon potentials, and Argonne v_{14} with the Tucson-Melbourne, Urbana VII, and Urbana VIII three-nucleon potentials. The variational binding energies are typically 3–4 % above available Faddeev and Green's-function Monte Carlo results. Nucleon density distributions and elastic electromagnetic form factors are also presented. Extension of these wave functions to larger nuclei such as ^{5}He, ^{6}He, and ^{6}Li is discussed.

I. INTRODUCTION

A major problem in nuclear physics is understanding how nuclear structure comes about from the underlying interactions between nucleons. This requires modeling nuclei as collections of strongly interacting nucleons. There are many fundamental issues that have not been addressed satisfactorily to date, including the stability of light nuclei against breakup and the origin of the spin-orbit splitting. A starting point for resolving these issues is the solution of the many-body Schrödinger equation $H\Psi = E\Psi$ for realistic nuclear Hamiltonians such as

$$H = \sum_i \frac{-\hbar^2}{2m}\nabla_i^2 + \sum_{i<j} v_{ij} + \sum_{i<j<k} V_{ijk} \ , \tag{1.1}$$

where v_{ij} is a nucleon-nucleon potential that fits scattering data and deuteron properties and V_{ijk} is a supplemental three-nucleon potential.

Many realistic nucleon-nucleon potentials can be written in an operator form:

$$v_{ij} = \sum_{p=1}^{n} v_p(r_{ij}) O_{ij}^p \ , \tag{1.2}$$

where

$$\begin{aligned} O_{ij}^{p=1,14} = & 1, \tau_i\cdot\tau_j, \sigma_i\cdot\sigma_j, (\sigma_i\cdot\sigma_j)(\tau_i\cdot\tau_j), S_{ij} \ , \\ & S_{ij}(\tau_i\cdot\tau_j), \mathbf{L}\cdot\mathbf{S}, \mathbf{L}\cdot\mathbf{S}(\tau_i\cdot\tau_j), L^2 \ , \\ & L^2(\tau_i\cdot\tau_j), L^2(\sigma_i\cdot\sigma_j), L^2(\sigma_i\cdot\sigma_j)(\tau_i\cdot\tau_j) \ , \\ & (\mathbf{L}\cdot\mathbf{S})^2, (\mathbf{L}\cdot\mathbf{S})^2(\tau_i\cdot\tau_j) \ . \end{aligned} \tag{1.3}$$

(For convenience, we sometimes refer to these operators by the abbreviations c, τ, σ, $\sigma\tau$, t, $t\tau$, b, $b\tau$, q, $q\tau$, $q\sigma$, $q\sigma\tau$, bb, and $bb\tau$). The first eight operators appear in the Reid v_8 potential,[1] while all 14 terms appear in the Argonne v_{14} potential.[2] In several other potential models, such as Paris,[3] the four terms with L^2 operators are replaced by similar terms with p^2 operators. Models for the three-nucleon potential V_{ijk} commonly include a long-range two-pion-exchange part of the Fujita–Miyazawa form,[4] and may also include short-range parts as in the Tucson-Melbourne model[5] and Urbana models.[6,7]

The variational method can be used to obtain approximate solutions to the many-body Schrödinger equation for a wide range of nuclear systems, from few-body nuclei[6–8] such as ^{3}H and ^{4}He, to light nuclei[9] such as ^{16}O, to nuclear matter and neutron stars.[10–12] A suitably parametrized trial function Ψ_v is used to calculate an upper bound to the energy:

$$E_v = \frac{\langle \Psi_v | H | \Psi_v \rangle}{\langle \Psi_v | \Psi_v \rangle} \geq E_0 \ . \tag{1.4}$$

The parameters in Ψ_v are varied to minimize E_v, and the lowest value is taken as the approximate ground-state energy. The corresponding Ψ_v can then be used to calculate other properties, such as the particle density, momentum distributions,[7] and electromagnetic form factors.[13,14] The quality of such calculations depends on the chosen form of the variational function Ψ_v and the accuracy with which the expectation value is evaluated.

A general form for the trial function that has been used in few-body nuclei and nucleon matter is a symmetrized product of two-body correlation operators $(1+U_{ij})$ acting on a Jastrow trial function:

$$|\Psi_v\rangle = \left[S \prod_{i<j} (1+U_{ij}) \right] |\Psi_J\rangle \ , \tag{1.5}$$

where

$$|\Psi_J\rangle = \prod_{i<j} f_c(r_{ij}) |\Phi\rangle \ . \tag{1.6}$$

Here $f_c(r)$ is a central pair-correlation function and Φ is

an appropriate antisymmetric single-particle wave function. The philosophy behind this ansatz is that each operator component of the two-body interaction can induce a corresponding correlation in the wave function. Hence a standard choice for the pair-correlation operator is

$$U_{ij}=\sum_{p=2}^{m} u_p(r_{ij})O_{ij}^p \tag{1.7}$$

where the number of operators m is as large a subset of the potential operators of Eq. (1.3) as can be conveniently used in a calculation. The symmetrization is required because the operators do not commute. In nuclear matter and ^{16}O, for example, the first eight operators have been used, although expectation values involving spin-orbit correlations are evaluated at a lower level than spin, isospin, and tensor correlations.

Most previous variational calculations of few-body nuclei using operator-product trial functions have used a simpler pair-correlation operator $\bar{U}_{ij}$ containing only two noncentral terms:

$$\bar{U}_{ij}=u_\sigma(r_{ij})\sigma_i\cdot\sigma_j+u_{t\tau}(r_{ij})S_{ij}(\tau_i\cdot\tau_j)\ . \tag{1.8}$$

This simpler form gives a reasonably good trial function for the s-shell nuclei because[15] up to terms linear in u_p it is equivalent to the U_{ij} of Eq. (1.7) with $m=8$. The $\bar{U}_{ij}$ is constructed from knowledge of the S-wave nucleon-nucleon interactions, and thus is a sort of variational equivalent of the standard five-channel Faddeev wave function. In previous calculations and the current work, a central three-body correlation is generally folded into the $u_p(r_{ij})$:

$$u_p(r_{ij})\rightarrow\left[\prod_{k\neq i,j} f_{ijk}\right]u_p(r_{ij})\ . \tag{1.9}$$

In this article we construct variational trial functions for few-body nuclei of the form

$$|\Psi_v\rangle=\left[1+\sum_{i<j}U_{ij}^{LS}+\sum_{i<j<k}U_{ijk}^{\mathrm{TNI}}\right]\times\left[S\prod_{i<j}(1+U_{ij})\right]|\Psi_J\rangle\ , \tag{1.10}$$

where U_{ij} contains the first five noncentral operators of Eq. (1.3) and U_{ij}^{LS} is the spin-orbit correlation operator,

$$U_{ij}^{LS}=\beta\sum_{p=7}^{8}u_p(r_{ij})O_{ij}^p\ , \tag{1.11}$$

with β a simple multiplicative constant. It would be preferable to include spin-orbit correlations in the product form, i.e., as part of Eq. (1.7), but then expectation values would be much more expensive to compute. The U_{ijk}^{TNI} is a three-body correlation induced by the three-nucleon interaction V_{ijk} and has a correspondingly complex operator dependence.

The effect of these three improvements to the trial functions used in Refs. 6–8 for few-body nuclei, i.e., the increase to five noncentral operators in U_{ij}, and the addition of U_{ij}^{LS} and U_{ijk}^{TNI}, is systematically studied here by calculating the ground-state binding energies of ^{3}H and ^{4}He with three Hamiltonians: the Reid v_8 and Argonne v_{14} two-nucleon potentials, and Argonne v_{14} with the Urbana VII three-nucleon potential. Additional calculations for the Urbana VIII and Tucson-Melbourne three-nucleon potentials are also reported. Expectation values are obtained using the Metropolis Monte Carlo algorithm.[16] Essentially exact Faddeev calculations[17] have been made for ^{3}H with these Hamiltonians, and Green's-function Monte Carlo results[18] are available for ^{4}He with Reid v_8 and for Argonne v_{14} + Urbana VIII. The best trial functions of the old form, using $\bar{U}_{ij}$ without U_{ij}^{LS} or U_{ijk}^{TNI} terms, give upper-bound energies that are typically 7–8 % above the exact results. The new trial functions reported here give upper bounds that are typically 3–4 % above the exact results.

The method for generating the pair correlations $f_c(r)$ and $u_p(r)$ and their parametrization is presented in Sec. II along with the triplet correlations. The method of evaluating expectation values and searching parameter space for the best trial function is explained in Sec. III. Section IV contains numerical results for the various Hamiltonians. Section V discusses a reasonable extension of this wave function for five- and six-body nuclei. A discussion and conclusions are given in Sec. VI.

II. PAIR AND TRIPLET CORRELATIONS

The pair correlation should reflect the influence of the two-body potential at short distances, while satisfying asymptotic boundary conditions of single-particle separability. Reasonable correlations can be generated[11] by minimizing the two-body cluster energy of an interaction $(\bar{v}-\lambda)$. The quenched interaction $\bar{v}$ is related to the bare interaction by

$$\bar{v}_{ij}=\sum_{p=1}^{n}\alpha_p v_p(r_{ij})O_{ij}^p\ , \tag{2.1}$$

where the variational parameters α_p are meant to simulate the average quenching of spin-isospin interactions between particles i and j due to interactions of these particles with others in the system. The Lagrange multipliers $\lambda_p(r)$ simulate screening effects at short distances, and are fixed at large distances by the asymptotic behavior of the correlation functions.

Eight coupled differential equations are needed to generate the eight pair-correlation functions $f_c(r)$ and $u_p(r)$, where $p=2$–8. By projecting into channels of fixed spin, S, and isospin, T, the equations can be decoupled to two single-channel equations for $T=0,1$ and $S=0$ states, and two triple-channel equations for $T=0,1$ and $S=1$ states. These channel equations are written in terms of four central functions $f_{S,T}(r)$, two tensor functions $f_{t,T}(r)$, and two spin-orbit functions $f_{b,T}(r)$. The differential equations have been previously derived for v_8 and v_{14} potentials in nuclear matter at fixed density.[10,11] In the present work, we use the same equations, but in the limit $k_F\rightarrow 0$. The single-channel equation for $S=0$ states (with $L=0$ for $T=1$, the $^1S_0$ state, and $L=1$ for $T=0$, the $^1P_1$ state) is

$$-\frac{\hbar^2}{m}\left[(f_{0,T}r^{L+1})''-\frac{L(L+1)}{r^2}(f_{0,T}r^{L+1})\right]+[\bar{v}_{0,T}+\lambda_{0,T}+L(L+1)\bar{v}_{q0,T}](f_{0,T}r^{L+1})=0\ , \tag{2.2}$$

where the double prime denotes a second derivative. The three coupled channels for $S=1$ states (with $L=0$ for $T=0$, the $^3S_1$-$^3D_1$ states, and $L=1$ for $T=1$, the $^3P_2$-$^3F_2$ states) are

$$-\frac{\hbar^2}{m}\left[(f_{1,T}r^{L+1})''-\frac{L(L+1)}{r^2}(f_{1,T}r^{L+1})\right]+[\bar{v}_{1,T}+\lambda_{1,T}+L(L+1)(\bar{v}_{q1,T}+\tfrac{2}{3}\bar{v}_{bb,T})](f_{1,T}r^{L+1})$$
$$+8[\bar{v}_{t,T}+\lambda_{t,T}-\tfrac{1}{12}L(L+1)\bar{v}_{bb,T}](f_{t,T}r^{L+1})+\tfrac{2}{3}L(L+1)(\bar{v}_{b,T}+\lambda_{b,T}-\tfrac{1}{2}\bar{v}_{bb,T})(f_{b,T}r^{L+1})=0\ , \tag{2.3}$$

$$-\frac{\hbar^2}{m}\left[(f_{t,T}r^{L+1})''-\frac{6+L(L+1)}{r^2}(f_{t,T}r^{L+1})\right]+[\bar{v}_{t,T}+\lambda_{t,T}-\tfrac{1}{12}L(L+1)\bar{v}_{bb,T}](f_{1,T}r^{L+1})$$
$$+[\bar{v}_{1,T}+\lambda_{1,T}-2(\bar{v}_{t,T}+\lambda_{t,T})-3(\bar{v}_{b,T}+\lambda_{b,T})+6\bar{v}_{q1,T}+9\bar{v}_{bb,T}+L(L+1)(\bar{v}_{q1,T}+\tfrac{5}{6}\bar{v}_{bb,T})]$$
$$\times(f_{t,T}r^{L+1})-\tfrac{1}{12}L(L+1)(\bar{v}_{b,T}+\lambda_{b,T}-2\bar{v}_{bb,T})(f_{b,T}r^{L+1})=0\ , \tag{2.4}$$

and

$$-\frac{\hbar^2}{m}\left[(f_{b,T}r^{3-L})''-\frac{6-4L}{r^2}(f_{b,T}r^{3-L})\right]+(\bar{v}_{b,T}+\lambda_{b,T}-\tfrac{1}{2}\bar{v}_{bb,T})(f_{1,T}r^{3-L})-(\bar{v}_{b,T}+\lambda_{b,T}-2\bar{v}_{bb,T})(f_{t,T}r^{3-L})$$
$$+[\bar{v}_{1,T}+\lambda_{1,T}-(\bar{v}_{t,T}+\lambda_{t,T})-\tfrac{1}{2}(\bar{v}_{b,T}+\lambda_{b,T})+(6-4L)(\bar{v}_{q1,T}+\bar{v}_{bb,T})](f_{b,T}r^{3-L})=0\ . \tag{2.5}$$

For finite nuclei, the boundary conditions imposed on $f_{S,T}$, $f_{t,T}$, and $f_{b,T}$ are

$$f_{S,T}(r\to 0)=\text{constant}\ ,$$
$$f_{S,T}(r\to\infty)=h_{S,T}\left[\frac{\exp(-k_{S,T}r)}{r}\right]^{1/(A-1)}\ ,$$
$$f_{t,T}(r\to 0)=0\ ,$$
$$f_{t,T}(r\to\infty)=\eta_T T(r) f_{S,T}(r)\ ,$$
$$f_{b,T}(r\to 0)=\text{constant}\ ,$$
$$f_{b,T}(r\to\infty)=\zeta_T B(r) f_{S,T}(r)\ , \tag{2.6}$$

where

$$T(r)=\left[1+\frac{3}{k_{S,T}r}+\frac{3}{(k_{S,T}r)^2}\right]\times\{1-\exp[-(r/d_{t,T})^2]\}\ ,$$
$$B(r)=\left[\frac{1}{r^2}+\frac{k_{S,T}}{r}\right]\{1-\exp[-(r/d_{b,T})^2]\}\ , \tag{2.7}$$
$$k_{S,T}=\left[\frac{A-1}{A}\frac{2m}{\hbar^2}E_{S,T}\right]^{1/2}\ .$$

The asymptotic boundary conditions imposed on the f_x are suggested by previous work[6–8] which examined the wave function when one nucleon is separated far from the other $A-1$ nucleons. The separation energies $E_{S,T}$, normalizations $h_{S,T}$, tensor/central ratios η_T, and spin-orbit/central ratios ζ_T are variational parameters. The Lagrange multipliers λ_x in Eqs. (2.2)–(2.5) are radial functions consisting of two parts: The long-range part $\Lambda_x(r)$ is fixed by the asymptotic behavior of f_x and is cut off at short distances by an exponential function, while the short-range part is a Woods–Saxon function multiplied by a constant Γ_x:

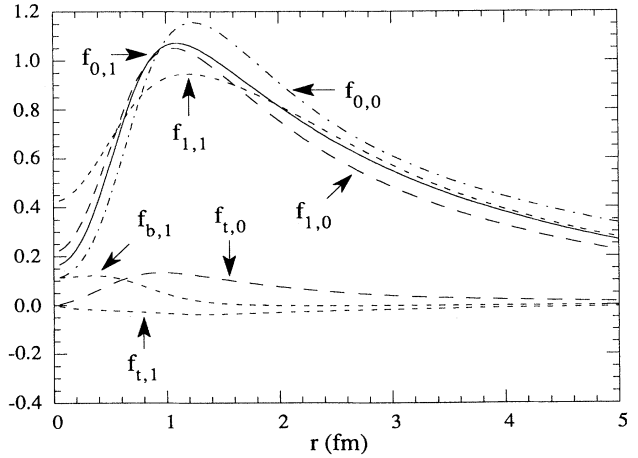

FIG. 1. The $f_{S,T}(r)$, $f_{t,T}(r)$, and $f_{b,1}(r)$ correlations for ^{4}He Argonne v_{14} + Urbana VIII Hamiltonian.

$$\lambda_x=\Gamma_x\left[1+\exp\left[\frac{r-R_x}{a_x}\right]\right]^{-1}$$
$$+\Lambda_x(r)\{1-\exp[-(r/c_x)^2]\}\ . \tag{2.8}$$

The constants Γ_x are determined by solving the differential equations subject to the boundary conditions. The Woods–Saxon and exponential cutoff constants R_x, a_x, and c_x in Eq. (2.8) and the exponential cutoff constants d_x in the tensor and spin-orbit functions $T(r)$ and $B(r)$ of Eq. (2.7) are additional variational parameters.

The functions $f_c(r)$ and $u_p(r)$ in the operators U_{ij} and U_{ij}^{LS} are related to the channel functions via

$$\sum_{S,T} f_{S,T}(r_{ij})P_SP_T=\sum_{p=1}^{4} f_p(r_{ij})O_{ij}^p$$
$$=f_c(r_{ij})\left[1+\sum_{p=2}^{4}u_p(r_{ij})O_{ij}^p\right]\ ,$$
$$\sum_{T} f_{t,T}(r_{ij})S_{ij}P_T=\sum_{p=5}^{6} f_p(r_{ij})O_{ij}^p \tag{2.9}$$
$$=f_c(r_{ij})\sum_{p=5}^{6}u_p(r_{ij})O_{ij}^p\ ,$$
$$\sum_{T} f_{b,T}(r_{ij})(\mathbf{L}\cdot\mathbf{S})P_T=\sum_{p=7}^{8} f_p(r_{ij})O_{ij}^p$$
$$=f_c(r_{ij})\sum_{p=7}^{8}u_p(r_{ij})O_{ij}^p\ ,$$

where P_S and P_T are the usual spin and isospin projection operators, i.e., $P_{S=1}=(3+\sigma_i\cdot\sigma_j)/4$, $P_{S=0}=(1-\sigma_i\cdot\sigma_j)/4$, etc. The optimized $f_{S,T}(r)$, $f_{t,T}(r_{ij})$, and $f_{b,T}(r_{ij})$ for ^{4}He with the Argonne v_{14} plus Urbana VIII Hamiltonian are shown in Fig. 1. The corresponding operator functions $f_c(r)$ and $u_p(r)$ are shown in Fig. 2. A comparison of the $f_c(r)$ and $u_{t\tau}(r)$ for ^{2}H, ^{3}H, and ^{4}H is given in Fig. 3.

The total number of possible parameters in these equations is 54, which includes 14 α_p to define $\bar{v}$, 8 values each for the parameters R_x, a_x, and c_x in λ, 4 values for the asymptotic cutoffs d_x, 8 values for the asymptotic strengths $E_{S,T}$, η_T, and ζ_T, and 4 values for the mixing parameters $h_{S,T}$. In practice far fewer are used. The α_p are taken to be 1 for $p=1,9,13,14$, and a single value α for all other p. Four values of R_x are used: $R_0=R_{S=0,T}$, $R_1=R_{S=1,T}$, $R_t=R_{t,T}$, and $R_b=R_{b,T}$. Only two values of a_x are used: $a=a_{S,T}=a_{t,T}$ and $a_b=a_{b,T}$; two values of c_x: $c_0=c_{S=0,T}$ and $c_1=c_{S=1,T}=c_{t,T}=c_{b,T}$; and a single value of d_x; $d=d_{t,T}=d_{b,T}$. In addition, there is the multiplicative constant β in Eq. (1.11).

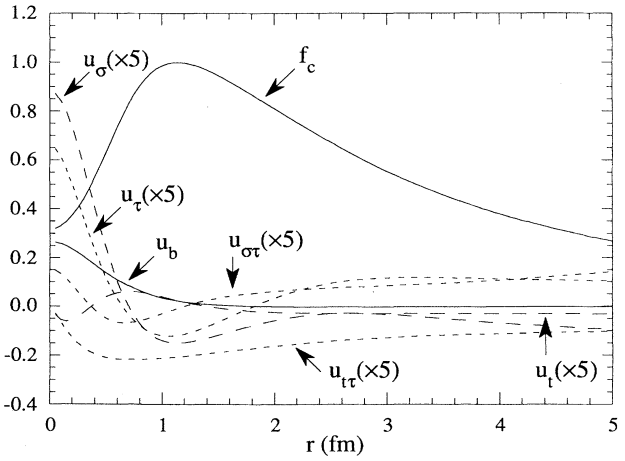

FIG. 2. The projected $f_c(r)$ and $u_p(r)$ correlations for ^{4}He with the Argonne v_{14}+Urbana VIII Hamiltonian.

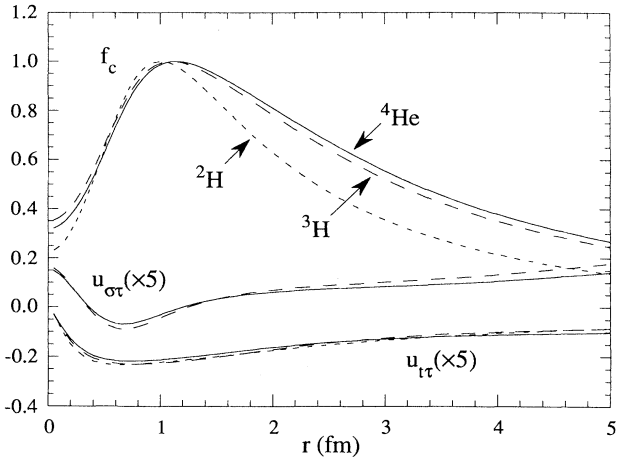

FIG. 3. The $f_c(r)$, $u_{\sigma\tau}(r)$, and $u_{t\tau}(r)$ correlations for ^{2}H, ^{3}H, and ^{4}He with the Argonne v_{14}+Urbana VIII Hamiltonian.

In practice, the addition of a spin-orbit correlation in the $S=1$, $T=0$ ($^3S_1$-$^3D_1$) channel was found not to improve the energy of the trial function, so $f_{b,0}$ is taken to be zero and no ζ_0 parameter is required. This is not surprising, since there is no direct coupling of central and tensor channels to the spin-orbit correlation in Eqs. (2.3) and (2.4) for $L=0$. Further, the energies are not very sensitive to the cutoff parameters a, a_b, c_0, c_1, and d. One set of values was used for all the Hamiltonians studied in both ^{3}H and ^{4}He: $a=0.4$, $a_b=0.3$, $c_0=1.0$, $c_1=3.0$, and $d=2.0$ fm. The remaining 17 pair-correlation parameters for the best trial functions found are given in Table I for ^{3}H, and in Table II for ^{4}He.

The $\bar{U}_{ij}$ of Eq. (1.8) used in the earlier variational calculations[6–8] can be constructed as a special case of the equations used here. If Eqs. (2.2)–(2.4) are solved only in $L=0$ channels, i.e., for $(S,T)=(0,1)$ and (1,0), then operator components f_c, u_σ, and $u_{t\tau}$ can be projected by the expressions

$$f_c=\tfrac{1}{4}(3f_{1,0}+f_{0,1})\ ,$$
$$u_\sigma=\tfrac{1}{4}(f_{1,0}-f_{0,1})/f_c\ ,$$
$$u_{t\tau}=-\tfrac{1}{3}f_{t,0}/f_c\ . \tag{2.10}$$

In practice, this will give correlations only marginally different from those used in earlier work, and will serve

TABLE I. Pair- and triplet-correlation parameters for ^{3}H. Energies $E_{S,T}$ are in MeV and radii R_x are in fm. All other parameters are dimensionless.

Hamiltonian	Reid v_8	Argonne v_{14}	Argonne v_{14} +Tucson	Argonne v_{14} +Urbana VII	Argonne v_{14} +Urbana VIII
$E_{0,0}$	1.8	1.6	2.0	2.6	2.4
$E_{0,1}$	5.4	5.4	6.8	7.2	7.0
$E_{1,0}$	12.0	10.8	13.0	12.2	12.0
$E_{1,1}$	5.8	4.8	5.4	7.0	6.8
$h_{0,0}$	1.81	1.37	1.42	1.45	1.43
$h_{0,1}$	1.77	1.82	1.86	1.90	1.90
$h_{1,0}$	1.86	1.89	2.02	1.94	1.88
$h_{1,1}$	1.79	1.69	1.73	1.83	1.83
η_0	0.026	0.027	0.027	0.028	0.028
η_1	−0.008	−0.006	−0.009	−0.009	−0.009
ζ_1	0.001	−0.020	−0.020	−0.020	−0.020
α	0.94	0.93	0.90	0.91	0.92
R_0	0.8	0.8	0.8	0.8	0.8
R_1	2.8	2.8	2.8	2.8	2.8
R_t	3.4	3.2	3.6	3.6	3.6
R_b	0.8	0.6	0.8	0.8	0.8
β	0.5	0.4	0.5	0.5	0.5
t_1	10.0	10.0	9.0	8.0	8.0
ϵ			−0.000 15	−0.0004	−0.0004
b			0.70	0.70	0.70

as a reference point for the new correlations of the present work.

There are two kinds of triplet correlations in the trial function of Eq. (1.10). There is the central three-body correlation f_{ijk} in expression (1.9), which modifies the noncentral pair-correlation operators $u_p(r_{ij})$, and there is the three-body correlation operator U_{ijk}^{TNI} representing the correlations induced by V_{ijk}. The f_{ijk} performs a quenching function analogous to the potential quencher α_p of Eq. (2.1), but in a manner that is dependent on the relative position of a third particle with a correlated pair. It is used whether or not there is a V_{ijk} term in the Hamiltonian. The same form is chosen here that has appeared in previous work,[7]

TABLE II. Pair- and triplet-correlation parameters for ^{4}He. Energies $E_{S,T}$ are in MeV and radii R_x are in fm. All other parameters are dimensionless.

Hamiltonian	Reid v_8	Argonne v_{14}	Argonne v_{14} +Tucson	Argonne v_{14} +Urbana VII	Argonne v_{14} +Urbana VIII
$E_{0,0}$	11.0	7.0	9.0	11.0	9.0
$E_{0,1}$	18.0	16.0	22.0	22.0	20.0
$E_{1,0}$	21.0	20.0	26.0	26.0	23.0
$E_{1,1}$	17.0	15.0	18.0	19.0	17.0
$h_{0,0}$	2.05	1.41	1.47	1.51	1.47
$h_{0,1}$	1.77	1.78	1.91	1.91	1.88
$h_{1,0}$	1.76	1.75	1.83	1.85	1.75
$h_{1,1}$	1.72	1.70	1.76	1.79	1.74
η_0	0.040	0.040	0.038	0.039	0.038
η_1	−0.014	−0.014	−0.014	−0.017	−0.014
ζ_1	0.001	−0.020	−0.020	−0.020	−0.020
α	0.84	0.78	0.82	0.82	0.82
R_0	0.8	0.8	0.8	0.8	0.8
R_1	2.8	2.8	2.8	2.8	2.8
R_t	3.4	3.2	3.6	3.6	3.6
R_b	0.8	0.6	0.8	0.8	0.8
β	0.4	0.5	0.5	0.5	0.5
t_1	13.0	11.0	9.0	8.0	9.0
ϵ			−0.000 15	−0.0004	−0.0004
b			0.70	0.70	0.70

$$f_{ijk}=1-t_1\left[\frac{r_{ij}}{R_{ijk}}\right]^{t_2}\exp(-t_3R_{ijk})\ , \tag{2.11}$$

where $R_{ijk}=r_{ij}+r_{jk}+r_{ki}$. The t_1, t_2 and t_3 are variational parameters and could in principle be made different for each $u_p(r)$ in expression (1.9), but a single set of three parameters is used here.

The $U_{ijk}^{\rm TNI}$ is used only when a V_{ijk} term is present in the Hamiltonian. Its form is suggested by simple perturbation theory:

$$U_{ijk}^{\rm TNI}=\epsilon V_{ijk}(\overline{r}_{ij},\overline{r}_{jk},\overline{r}_{ki})\ . \tag{2.12}$$

Here $\overline{r}=br$ is a scaled variable that serves to spread out the correlation relative to the interaction and ϵ is a small negative multiplicative constant. This form builds into $U_{ijk}^{\rm TNI}$ all the operator dependence of the three-nucleon interaction. For example, the Urbana series of three-nucleon potential models[6,7] is given by a sum of long-range two-pion-exchange and intermediate-range repulsive terms:

$$V_{ijk}=V_{ijk}^{2\pi}+V_{ijk}^{R}\ . \tag{2.13}$$

Here the two-pion-exchange part is a cyclic sum over indices ij, jk, and ki of products of anticommutator and commutator terms:

$$V_{ijk}^{2\pi}=\sum_{\rm cyc}A(\{X_{ij},X_{jk}\}\{\tau_i\cdot\tau_j,\tau_j\cdot\tau_k\} +\tfrac{1}{4}[X_{ij},X_{jk}][\tau_i\cdot\tau_j,\tau_j\cdot\tau_k])\ , \tag{2.14}$$

where $X_{ij}=Y(r_{ij})\sigma_i\cdot\sigma_j+T(r_{ij})S_{ij}$ is the one-pion-exchange operator. The intermediate-range repulsion is a cyclic sum of purely central character:

$$V_{ijk}^{R}=\sum_{\rm cyc}UT^2(r_{ij})T^2(r_{jk})\ . \tag{2.15}$$

The potential constants A and U have the values -0.0333 and 0.0038 in Urbana model VII, and the values -0.028 and 0.005 in Urbana model VIII. The Tucson-Melbourne three-nucleon potential[5] has a more general two-pion-exchange part with additional operator terms, but no intermediate-range repulsive part. In either case, $U_{ijk}^{\rm TNI}$ has the full operator dependence of the interaction.

This kind of three-nucleon correlation was tried in earlier work[6] in the case of ^{3}H, but with the scale factor $b=1$, so the correlation was not spread out. That correlation gave an improvement that was statistically insignificant. With $b<1$ and the energy-difference techniques described below, the scaled correlation gives a clear improvement in ^{3}H and has a very significant effect in ^{4}He.

In practice, the parameters t_2 and t_3 in Eq. (2.11) are taken to be the same for all Hamiltonians in both ^{3}H and ^{4}He: $t_2=4$ and $t_3=0.1$ fm^{-1}. The optimal values of the remaining three parameters, t_1 from Eq. (2.11) and ϵ and b from Eq. (2.12) are given along with the pair-correlation parameters in Tables I and II.

III. ENERGY EVALUATIONS AND PARAMETER SEARCHES

Energy expectation values are calculated using Monte Carlo integration.[8,19] The expectation values are sampled both in configuration space and in the order of operators in the symmetrized product of Eq. (1.10) by following a Metropolis random walk.[16] Sampling in the order of operators saves significant computational effort, since the number of possible orders is $P!$, where $P=\frac{1}{2}A(A-1)$ is the number of pairs. This introduces relatively little statistical variance, because the different orders contain the same linear terms and differ only at $O(u_p^2)$ and above.

The Monte Carlo energy expectation value is given by

$$\langle H\rangle=\frac{\sum\langle\Psi_p^\dagger(\mathbf{R})H\Psi_q(\mathbf{R})\rangle/W_{pq}(\mathbf{R})}{\sum\langle\Psi_p^\dagger(\mathbf{R})\Psi_q(\mathbf{R})\rangle/W_{pq}(\mathbf{R})} \tag{3.1}$$

where the sums run over configurations denoted by the particle coordinate set $\mathbf{R}=(\mathbf{r}_1,\mathbf{r}_2,\ldots,\mathbf{r}_A)$, and the specific order of operators, p and q, on the left and right sides. The brackets indicate a complete sum over all spin-isospin variables. The weight function is

$$W_{pq}(\mathbf{R})={\rm Re}(\langle\Psi_p^\dagger(\mathbf{R})\Psi_q(\mathbf{R})\rangle)\ . \tag{3.2}$$

The Metropolis algorithm produces a set of configurations $\{\mathbf{R},p,q\}$ whose density is proportional to this probability distribution. The energy evaluation has a statistical error, estimated by the standard deviation σ:

$$\sigma=\left[\frac{\langle H^2\rangle-\langle H\rangle^2}{N-1}\right]^{1/2}\ , \tag{3.3}$$

where N is the number of statistically independent samples.

The wave function Ψ can be represented by an array of $2^A\times\binom{A}{Z}$ complex numbers, which are the coefficients of each state with specific third components of spin and isospin. The spin, isospin, and tensor operators $O_{ij}^{p=2,6}$ contained in the two-body correlation operator U_{ij} and in the Hamiltonian are sparse matrices in this basis.[19]

The initial uncorrelated state, $\Phi=\Phi(JMTT_3)$, is taken to be an antisymmetrized product of single-particle spin-isospin states with no coordinate dependence:

$$\Phi(^3{\rm H})=\Phi_t(\tfrac{1}{2}\tfrac{1}{2}\tfrac{1}{2}-\tfrac{1}{2})=A\,|p\uparrow n\uparrow n\downarrow\rangle\ ,$$
$$\Phi(^4{\rm He})=\Phi_\alpha(0000)=A\,|p\uparrow p\downarrow n\uparrow n\downarrow\rangle\ . \tag{3.4}$$

The Jastrow wave function $\Psi_J(\mathbf{R})$ is obtained by multiplying Φ with the central pair correlations $f_c(r_{ij})$ for the coordinate set $\mathbf{R}$. The trial function of Eq. (1.5) is then built up by successive matrix multiplication with the pair-correlation operators U_{ij} (in the selected order p or q) on Ψ_J. This matrix multiplication is the basic unit of computational work, and is proportional to the size of the array. The construction of $\Psi_q(\mathbf{R})$ requires P of these matrix operations to build up the pair product, with another P operations to construct $\Psi_p(\mathbf{R})$.

The expectation value of the first six terms of the two-nucleon potential, $v_{p=1,6}$, are evaluated in a similar manner, with P sparse matrix operations required to sum

over the different pairs. The expectation values of the kinetic energy and spin-orbit potential terms require the computation of first derivatives and diagonal second derivatives of the wave function. These are obtained by moving each particle a small distance ϵ in both positive and negative directions along each axis:

$$\frac{\partial\Psi_q(\mathbf{R})}{\partial r_i^m}=\frac{1}{2\epsilon}[\Psi_q(\mathbf{R}+\epsilon r_i^m)-\Psi_q(\mathbf{R}-\epsilon r_i^m)]\ ,$$

$$\frac{\partial^2\Psi_q(\mathbf{R})}{\partial(r_i^m)^2}=\frac{1}{\epsilon^2}[\Psi_q(\mathbf{R}+\epsilon r_i^m)-2\Psi_q(\mathbf{R})+\Psi_q(\mathbf{R}-\epsilon r_i^m)]\ , \tag{3.5}$$

where r_i^m is the mth spatial component of particle coordinate $\mathbf{r}_i$. This requires $6A$ constructions of Ψ_q and is correct to $O(\epsilon^3)$. Potential terms quadratic in $\mathbf{L}$, such as those appearing in Argonne v_{14}, require mixed second derivatives:

$$\begin{aligned}\frac{\partial^2\Psi_q(\mathbf{R})}{\partial r_i^m\partial r_i^n}&=\frac{1}{\epsilon^2}[\Psi_q(\mathbf{R}+\epsilon r_i^m+\epsilon r_i^n)-\Psi_q(\mathbf{R}+\epsilon r_i^m)\\&\quad-\Psi_q(\mathbf{R}+\epsilon r_i^n)+\Psi_q(\mathbf{R})]\ ,\\\frac{\partial^2\Psi_q(\mathbf{R})}{\partial r_i^m\partial r_j^n}&=\frac{1}{\epsilon^2}[\Psi_q(\mathbf{R}+\epsilon r_i^m+\epsilon r_j^n)-\Psi_q(\mathbf{R}+\epsilon r_i^m)\\&\quad-\Psi_q(\mathbf{R}+\epsilon r_j^n)+\Psi_q(\mathbf{R})]\ ,\end{aligned} \tag{3.6}$$

which are calculated to $O(\epsilon^2)$ to save effort. Tests with derivatives calculated to $O(\epsilon^3)$ show this approximation to be sufficiently accurate for Argonne v_{14}, which has little net contribution from $v_{p=9,14}$ terms. These mixed second derivatives require an additional $3A+9P$ constructions of Ψ_q.

To evaluate the energy in one configuration for Ψ_v given by Eq. (1.5) with the Reid v_8 Hamiltonian requires the equivalent of $6A+3$ trial function constructions; for Argonne v_{14} the number is $9A+9P+3$. In addition there is the effort involved in generating statistically independent configurations proportional to $W_{pq}(\mathbf{R})$ through the Metropolis random walk. Typically 10 new configurations, with all the particles moved, are tested between each energy evaluation, requiring 20 more trial function constructions.

The spin-orbit correlation operators U_{ij}^{LS} require the same linear derivatives $\partial/\partial r_i^m$ as the spin-orbit potential. However, they must be evaluated more frequently, since they contribute to the weight function $W_{pq}(\mathbf{R})$ and well as to the energy expectation value. Because the $u_{p=7,8}$ are small, the derivatives are evaluated only to $O(\epsilon^2)$, requiring $3A$ (rather than $6A$) constructions of Ψ_p and $3A$ constructions of Ψ_q for each configuration $\{\mathbf{R},p,q\}$ tested in generating one sample $W_{pq}(\mathbf{R})$. Kinetic energy and potential terms quadratic in $\mathbf{L}$ involving the U_{ij}^{LS} are evaluated using integrations by parts, i.e., $\Psi_p(\mathbf{R})\overleftarrow{\nabla}_i\cdot\vec{\nabla}_i\Psi_q(\mathbf{R})$; this requires calculation of mixed second derivatives on both $\Psi_p(\mathbf{R})$ and $\Psi_q(\mathbf{R})$. Thus the introduction of spin-orbit correlations as in Eq. (1.10) adds significant computation to the generation of configurations $\{\mathbf{R},p,q\}$, and the energy evaluation.

The three-nucleon potential V_{ijk}, with the commutator and anticommutator structure of its two-pion-exchange part, Eq. (2.14), is evaluated using the same basic spin, isospin, and tensor sparse matrix operations required in the construction of U_{ij}. However, these operations must be made twice in opposite orders, and their results summed or differenced accordingly. Further, because of the cyclic sum over pairs, there are three such terms to evaluate in any given triple. Some effort can be saved by storing the results of the first operation on all pairs in a given triple, and using each as the starting point for two different terms in the cycling sum. The energy evaluation then requires $9T$ operations, where $T=\frac{1}{6}A(A-1)(A-2)$ is the number of triples.

The three-nucleon interaction correlations U_{ijk}^{TNI} require a similar effort to construct. However, they also contribute to the weight function $W_{pq}(\mathbf{R})$ and must be evaluated at every attempted move in the random walk. Evaluation of their kinetic energy and $\mathbf{L}$-dependent potential contributions also requires first derivatives and diagonal second derivatives and the corresponding wave function constructions at slightly shifted positions. Integrations by parts are used to avoid the necessity of evaluating mixed second derivatives for the U_{ijk}^{TNI}. This again requires that mixed second derivatives of both Ψ_p and Ψ_q be available, even if no U_{ij}^{LS} terms are used.

The computer time required to generate a statistically independent configuration $\{\mathbf{R},p,q\}$ and to evaluate its energy for the Argonne v_{14} plus Urbana VIII Hamiltonian is shown in Table III for systems ranging in size from $A=2$–6. These times have been measured on one processor of a Cray-YMP4; the approximate speed of the computer code and the memory requirements are also shown. The time required to sample the energy of the simple trial function of Eq. (1.5) is dominated by the kinetic-energy calculation. This is proportional to the number of wave-function constructions required for the kinetic energy, the number of pairs in the symmetrized product of correlations operators, and the size of the array for Ψ, or $A\times P\times 2^A\times\binom{A}{Z}$. This factor grows roughly 1 order of magnitude for each particle added to the system. It is compensated for somewhat by the increasing efficiency of the computer code as the relevant vectors get longer. For a given nucleus, the spin-orbit and three-nucleon interaction correlations add significantly to the computation effort, with the result that the full trial function of Eq. (1.10) requires almost 1 order of magnitude more time than the simple trial function of Eq. (1.5). This is partially compensated for by the fact that the full form is a fundamentally better trial function, with significantly less variance, and thus requires fewer samples to obtain an energy with the same Monte Carlo statistical error.

Two significant tests have been made to verify the computer code. The energy has been evaluated for ^{2}H using exact wave functions, and for ^{3}H using the 34-channel Faddeev wave functions of the Los Alamos–Iowa group.[17] For the deuteron, the exact wave function can be written in the correlation operator form of Eq. (1.5)

TABLE III. Computer time (in seconds) for generating one statistically independent configuration and evaluating its energy for different-size systems and different forms of the trial function. The Hamiltonian used here is Argonne v_{14} + Urbana VIII. The speed (in MFLOPS) and size (in Mwords) of the computer code is also shown.

	Ψ_v	Configuration	Energy	Total	Speed	Size
^{2}H	U_{ij}	0.0018	0.0006	0.0024	23	0.43
^{3}H	U_{ij}	0.0048	0.0032	0.0080	59	
	$U_{ij}+U_{ij}^{LS}+U_{ijk}^{\mathrm{TNI}}$	0.026	0.012	0.038	75	0.53
^{4}He	U_{ij}	0.013	0.024	0.037	120	
	$U_{ij}+U_{ij}^{LS}+U_{ijk}^{\mathrm{TNI}}$	0.15	0.11	0.26	118	0.65
^{5}He	U_{ij}	0.038	0.145	0.183	175	
	$U_{ij}+U_{ij}^{LS}+U_{ijk}^{\mathrm{TNI}}$	0.76	0.81	1.57	156	1.35
^{6}Li	U_{ij}	0.15	1.03	1.18	211	
	$U_{ij}+U_{ij}^{LS}+U_{ijk}^{\mathrm{TNI}}$	4.2	6.4	10.7	187	5.7

using $f_c(r)$ and $u_{t\tau}(r)$ correlations with the definitions[7]

$$f_c(r)=\frac{u(r)}{r},\quad u_{t\tau}(r)=\frac{-w(r)}{3\sqrt{8}u(r)}\ , \tag{3.7}$$

where $u(r)$ and $w(r)$ are the usual S- and D-wave deuteron wave functions. The deuteron energy and wave functions are found using an independent computer code, and the latter are used as input to the Monte Carlo energy expectation value code; the results agree within 1 keV. The configuration-space Faddeev wave functions for ^{3}H can also be used as input, and the energies reported below agree with those reported by the Los Alamos–Iowa group within 60 keV. Both these checks give some assurance that the energy expectation values are being accurately evaluated.

The search in parameter space for the best trial function of a given form is done by hand. The time required to evaluate an energy with a sufficiently small error estimate is too large to use an automated minimzation package that might make hundreds of evaluation requests. In earlier variational Monte Carlo calculations of few-body nuclei the standard procedure was to make many independent random walks with small changes in the wave function.[6–8] Unfortunately, the statistical errors of independent runs might be larger than the actual change in the energy, so promising routes to a lower energy might be missed. Also, there was a consequent tendency to pick a wave function whose energy had benefited from a low statistical fluctuation. With longer runs, the energy would almost inevitably go up.

In the present work the searching is done by evaluating energy differences between different trial functions using configurations generated by a single random walk. In general, the energy difference

$$\delta E=\tilde{E}-E=\frac{\sum\langle\tilde{\Psi}_p^{\dagger}(\mathbf{R})H\tilde{\Psi}_q(\mathbf{R})\rangle/W_{pq}(\mathbf{R})}{\sum\langle\tilde{\Psi}_p^{\dagger}(\mathbf{R})\tilde{\Psi}_q(\mathbf{R})\rangle/W_{pq}(\mathbf{R})}-\frac{\sum\langle\Psi_p^{\dagger}(\mathbf{R})H\Psi_q(\mathbf{R})\rangle/W_{pq}(\mathbf{R})}{\sum\langle\Psi_p^{\dagger}(\mathbf{R})\Psi_q(\mathbf{R})\rangle/W_{pq}(\mathbf{R})} \tag{3.8}$$

between trial functions $\tilde{\Psi}$ and Ψ has a much smaller statistical error for a given number of samples than the absolute energy for either. In practice, an initial random walk is made with trial function Ψ to generate a set of configurations and weights $W_{pq}(\mathbf{R})$, which are stored. Then on the order of 10 different $\tilde{\Psi}$ are tried, varying one or two parameters at a time, with the energy difference being calculated using the same $W_{pq}(\mathbf{R})$. The $\tilde{\Psi}$ that gives the lowest energy is then used to generate a new $\tilde{W}_{pq}(\mathbf{R})$, and the search is continued. This search procedure is less likely to go astray due to statistical fluctuations in the energy evaluations. It has the added advantage of saving significant computational effort because a stored random walk is being used most of the time; the time required to generate a new configuration (first column of Table III) is effectively eliminated.

IV. RESULTS FOR THREE- AND FOUR-BODY NUCLEI

Calculations have been performed for ^{3}H and ^{4}He using five Hamiltonians: the Reid v_8 and Argonne v_{14} two-nucleon potentials, and for Argonne v_{14} with the Tucson-Melbourne, Urbana VII, and Urbana VIII three-nucleon potentials. In the first two cases the calculations are done using three different trial functions: $\overline{U}_{ij}$, U_{ij}, and $U_{ij}+U_{ij}^{LS}$. For Argonne v_{14} plus Urbana VII the two combinations $U_{ij}+U_{ijk}^{\mathrm{TNI}}$ and $U_{ij}+U_{ik}^{LS}+U_{ijk}^{\mathrm{TNI}}$ are added. For Urbana VIII and Tucson-Melbourne only the fully combination $U_{ij}+U_{ij}^{LS}+U_{ijk}^{\mathrm{TNI}}$ is used. Calculations for ^{3}H have also been made using the 34-channel Faddeev wave functions of the Los Alamos–Iowa group,[17] as input to the Monte Carlo code.

The search in parameter space is made using the energy-difference techniques discussed above. The optimal parameters are found first for the U_{ij} trial function in ^{3}H for a given Hamiltonian, typically using runs with 10 000 configurations. The parameters R_0, R_1, and R_t are then fixed for the other trial functions with that Hamiltonian. All other parameters continue to be varied as the U_{ij}^{LS} and U_{ijk}^{TNI} correlations are added. The addition of U_{ij}^{LS} correlations fixes the parameters ζ_1, R_b, and β; they are such a small perturbation that the only other parameter that need be varied is t_1. The U_{ijk}^{TNI} correlations have a bigger effect, and small increases in the $E_{S,T}$ and

TABLE IV. Absolute energies, energy differences, and best energies by least-square fits (in MeV) for ^{3}H with Argonne v_{14} interaction. Numbers in parentheses give 1-standard-deviation Monte Carlo error estimates in the last digits.

Ψ_v	$\bar{U}_{ij}$	U_{ij}	$U_{ij}+U_{ij}^{LS}$	Faddeev
E	−7.154(26)	−7.434(21)	−7.453(22)	−7.699(16)
$E(\bar{U}_{ij})-E(\Psi_v)$	0.0	0.198(39)	0.254(36)	
$E(U_{ij})-E(\Psi_v)$	−0.257(38)	0.0	0.042(7)	
$E(U_{ij}+U_{ij}^{LS})-E(\Psi_v)$	−0.293(34)	−0.032(13)	0.0	0.212(56)
E(Faddeev)$-E(\Psi_v)$			−0.330(57)	0.0
$E_{\rm fit}$	−7.173(17)	−7.415(13)	−7.454(13)	−7.702(15)

η_T parameters are generally beneficial. Going from ^{3}H to ^{4}He the parameters R_0, R_1, R_t, and R_b are kept fixed, and searching is done with runs of 5000 configurations. The major changes are a significant increase in the separation-energy parameters $E_{S,T}$ and η_T and a decrease in α.

When the optimal trial function of any given type is obtained, a long energy evaluation with 50 000 (25 000) configurations is made in ^{3}H (^{4}He). In addition, several energy-difference evaluations using 10 000 (5000) independent configurations are made up to help pin down the effect of different terms in the trial function. An example is shown in Table IV for the case of ^{3}H with the Argonne v_{14} interaction. The results of the long runs are given in the first row of numbers; the numbers in parentheses are the 1-standard-deviation error estimates in the last digits quoted. The difference results are given in the following set of numbers, where the column heading indicates the type of trial function used to generate the random walk, and the row heading indicates the trial function whose energy difference with the original trial function was evaluated. Final energies are obtained by performing a least-squares fit to both the long independent runs and the difference runs. These numbers are given in the final row of the table.

In Table IV the energy with the $U_{ij}+U_{ij}^{LS}$ trial function is lower than that with U_{ij} alone, but the difference between the two numbers is not statistically significant after independent walks with 50 000 samples. However, the two difference runs with only 10 000 samples both show that the $U_{ij}+U_{ij}^{\rm LS}$ trial function is better by a statistically significant amount. The difference runs with $\bar{U}_{ij}$ also support this conclusion. The final numbers after least-squares fitting reflecting this fact, and the combination of long independent runs and shorter difference runs reduces the error estimate of the final numbers.

The results of all the calculations for ^{3}H are shown in Table V, and for ^{4}He in Table VI. The numbers quoted are the fitted values from independent energy and energy-difference runs, with the exception of the last row of Faddeev energies for ^{3}H from Ref. 17, and the Green's-function Monte Carlo (GFMC) energies for ^{4}He. From these tables one can see that $\bar{U}_{ij}$ correlations give energies that are 6–8 % above the available exact Faddeev[17] or GFMC (Ref. 18) calculations. (The $\bar{U}_{ij}$ values reported here are consistent with the variational results reported in Refs. 7 and 8.) The $U_{ij}+U_{ij}^{LS}$ correlations give a significant improvement for the Reid v_8 and Argonne v_{14} models, reducing the upper bound to 3–4 % above the exact results. For the Urbana V_{ijk} models, the $U_{ij}+U_{ij}^{LS}+U_{ijk}^{\rm TNI}$ correlation also gives results that are within 3–4 % of the exact results The ^{3}H result with the Tucson-Melbourne V_{ijk} is off by nearly 6%, but an older $\bar{U}_{ij}$ result[20] is off by 13 %. The Monte Carlo results for the Faddeev wave function are generally slightly lower than the values given in Ref. 17.

The change from $\bar{U}_{ij}$ to U_{ij} correlations is the variational equivalent of going from a 5- to an 18-channel Faddeev calculation, in that the former is constructed from information about the $^1S_0$ and $^3S_1$-$^3D_1$ parts of the interaction, while the latter adds information about the P-wave parts. Because the nucleons in s-shell nuclei interact mainly in S waves, the $\bar{U}_{ij}$ correlations do provide a very good first trial function. However, the U_{ij} correlations are no more expensive to compute, and do give a

TABLE V. Binding-energy results for ^{3}H in MeV. Numbers in parentheses are 1-standard-deviation estimates of the Monte Carlo statistical error in the last place.

Hamiltonian	Reid v_8	Argonne v_{14}	Argonne v_{14} +Tucson	Argonne v_{14} +Urbana VII	Argonne v_{14} +Urbana VIII
$\bar{U}_{ij}$	6.99(2)	7.17(2)		8.37(2)	
U_{ij}	7.26(2)	7.41(1)		8.48(2)	
$U_{ij}+U_{ij}^{LS}$	7.31(2)	7.45(1)		8.54(2)	
$U_{ij}+U_{ijk}^{\rm TNI}$				8.69(1)	
$U_{ij}+U_{ij}^{LS}+U_{ijk}^{\rm TNI}$			8.80(3)	8.79(1)	8.21(2)
Faddeev (MC)	7.59(2)	7.70(1)	9.33(2)	9.05(1)	8.49(1)
Faddeev (Ref. 17)	7.59	7.67	9.32	8.99	8.46

TABLE VI. Binding-energy results for ^{4}He in MeV. Numbers in parentheses are 1-standard-deviation estimates of the Monte Carlo statistical error in the last place.

Hamiltonian	Reid v_8	Argonne v_{14}	Argonne v_{14} +Tucson	Argonne v_{14} +Urbana VII	Argonne v_{14} +Urbana VIII
$\bar{U}_{ij}$	23.06(6)	22.98(5)		28.46(8)	
U_{ij}	23.43(6)	23.37(4)		28.73(6)	
$U_{ij}+U_{ij}^{LS}$	23.62(6)	23.54(4)		28.94(6)	
$U_{ij}+U_{ijk}^{\mathrm{TNI}}$				30.04(4)	
$U_{ij}+U_{ij}^{LS}+U_{ijk}^{\mathrm{TNI}}$			30.64(9)	30.51(4)	27.23(6)
GFMC	24.55(13)				28.3(2)

significant improvement.

The U_{ij}^{LS} correlations give a small but statistically significant additional improvement. Interestingly, the U_{ij}^{LS} seems to be more effective when joined with the U_{ijk}^{TNI} in the presence of a three-nucleon potential. In earlier Faddeev Monte Carlo studies[21] of ^{3}H the small P-state part of the wave function gave a rather large contribution to the expectation value of various V_{ijk} models. The main role of U_{ij}^{LS} is probably to improve this part of the wave function. The U_{ijk}^{TNI} correlation gives a very significant contribution when a three-nucleon interaction is present. The U_{ij}^{LS} and U_{ijk}^{TNI} correlations together lower the energy by more than 0.4 MeV/nucleon in ^{4}He. Although the cost of computing these correlations is nearly eight times as great as for U_{ij} alone in ^{4}He, the trial function is sufficiently better that its Monte Carlo variance is only $\frac{2}{3}$ as large, so that only $\frac{1}{2}$ as many configurations need be sampled to get the same statistical error estimate.

A detailed breakdown of the energy expectation value for the Argonne v_{14}+Urbana VIII Hamiltonian is given in Table VII. The results for ^{2}H are obtained both by direct integration and by Monte Carlo evaluation with the exact wave function. For ^{3}H Monte Carlo evaluations have been made for both the best variational wave function and the 34-channel Faddeev wave function. For ^{4}He a Monte Carlo evaluation of the best variational wave function is shown, along with results from a Green's-function Monte Carlo calculation.[18] The GFMC calculation was actually made for a v_8 version of the Argonne potential, and then corrected in perturbation theory for differences with the v_{14} model. D-state percentages and point rms radii are also given.

The proton density distributions of ^{3}H, ^{3}He, and ^{4}He are displayed in Fig. 4. The variational wave functions tend to give a higher density in the interior than the Faddeev or GFMC wave functions. The elastic electromagnetic form factors, $F_c(q)$ and $F_m(q)$, are shown in Figs. 5–9. The form factors have been calculated in impulse approximation, and with the inclusion of the exchange-current contributions discussed in Refs. 13 and 14. The exchange currents include both a "model-independent" part fixed by the two-nucleon interaction that consequently has no free parameters, and a "model-dependent" part that includes the currents associated with the $\rho\pi\gamma$,

TABLE VII. Energy breakdown for Argonne v_{14}+Urbana VIII: ^{2}H is evaluated in both direct and Monte Carlo (MC) integration with the exact wave functions, ^{3}H is evaluated by the Monte Carlo code for both variational (VMC) and Faddeev (FMC) wave functions, ^{4}He has been evaluated by the Monte Carlo code for the variational wave function (VMC), and Green's-function Monte Carlo (GFMC) results are also shown. Energies are in MeV and radii in fm.

System Calculation No. of samples	^{2}H Direct	^{2}H MC 150 000	^{3}H VMC 50 000	^{3}H FMC 50 000	^{4}He VMC 25 000	^{4}He GFMC
E	−2.225	−2.225(1)	−8.20(2)	−8.49(1)	−27.2(2)	−28.3(2)
T_i	19.19	19.05(11)	50.5(4)	49.4(3)	106.6(8)	113.3(20)
v_{ij}	−21.42	−21.27(11)	−57.7(4)	−56.9(3)	−129.7(7)	−136.5(20)
$v_{ij}(p=1,6)$	−20.80	−20.67(11)	−56.9(4)	−56.1(3)	−129.3(8)	−136.2(20)
v_{ij}^{π}	−22.42	−22.45(10)	−47.8(2)	−47.4(2)	−105.8(4)	−111.8(10)
$v_{ij}(p=7,14)$	−0.61	−0.60(4)	−0.8(1)	−0.8(1)	−0.4(2)	−0.3(10)
$v_{ij}(e^2/r_{ij})$			[0.66(1)]	[0.65(1)]	0.74(1)	0.75(1)
V_{ijk}			−0.96(3)	−0.99(2)	−4.84(9)	−5.8(3)
$V_{ijk}^{2\pi}$			−1.87(3)	−1.84(3)	−9.48(11)	−10.8(3)
V_{ijk}^{R}			0.92(2)	0.86(2)	4.73(8)	5.0(2)
D state (%)	6.07		9.54(1)	9.68(1)	15.5(1)	16.6(2)
$\langle r_p^2\rangle^{1/2}$	1.98	1.96(1)	1.59(1)	1.61(1)	1.47(1)	1.45(1)
$\langle r_n^2\rangle^{1/2}$	1.98	1.96(1)	1.71(1)	1.75(1)	1.47(1)	1.45(1)

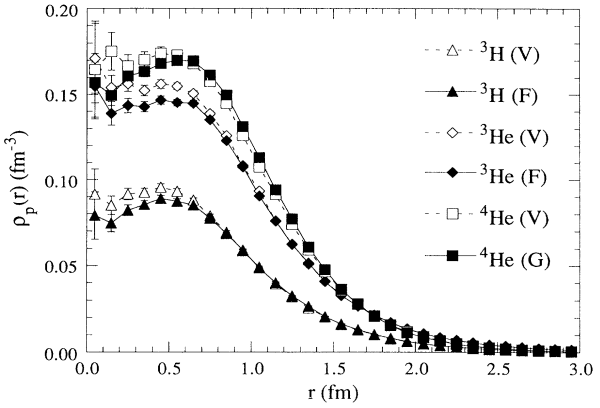

FIG. 4. Point proton density distributions for ^{3}H, ^{3}He, and ^{4}He with the Argonne v_{14}+Urbana VIII Hamiltonian in variational (V), Faddeev (F), and Green's-function Monte Carlo (G) calculations.

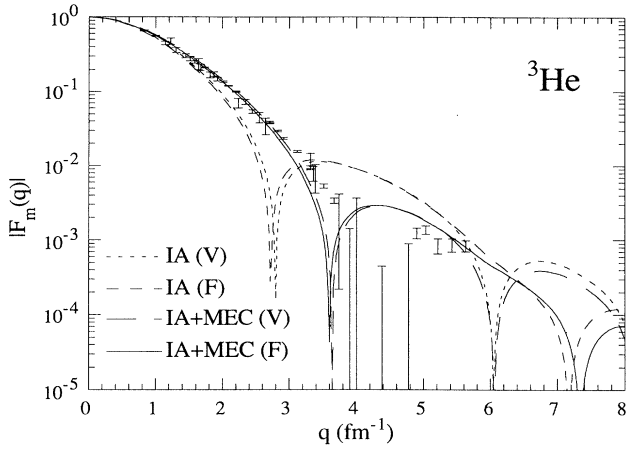

FIG. 6. Magnetic form factor $|F_m(q)|$ for ^{3}He with the Argonne v_{14}+Urbana VIII Hamiltonian calculated in impulse approximation (IA) and with meson-exchange-current (IA+MEC) contributions for both variational (V) and Faddeev (F) wave functions.

$\omega\pi\gamma$, and Δ-excitation mechanisms. The Höhler parametrization of the electromagnetic form factors of the nucleon is used.[22] The variational form factors have a first minimum at slightly larger wave number than the exact calculations, and a second minimum at smaller wave number. The corresponding magnetic moments for ^{3}H and ^{3}He are given in Table VIII.

The variational and Faddeev magnetic form factors for ^{3}H and ^{3}He are in reasonable agreement with data, although the position of the minimum is shifted toward lower q values. The magnetic moments are in good agreement with the experimental values. Retaining only the model-independent exchange currents would improve the agreement with the magnetic moments and form factors. The charge form factors for ^{3}H, ^{3}He, and ^{4}He are all in good agreement with data up to 6 fm^{-1}. Beyond about 7 fm^{-1} there are large Monte Carlo statistical errors in the expectation values and the differences between variational and exact calculations are not statistically significant. [It should be pointed out that the present Faddeev results for $F_m(q)$ and μ are somewhat different from those quoted in Ref. 14, where the wave function with the Urbana VII three-nucleon potential, which gives too much binding, was inadvertantly used instead of the Urbana VIII model.]

V. EXTENSION TO FIVE- AND SIX-BODY NUCLEI

The trial function of Eq. (1.10) can be used for larger nuclei by simply generalizing the structure of the Jastrow wave function Ψ_J. A Jastrow function for $A=5$ is constructed from an α-particle core with a fifth particle in a p-wave orbital with respect to that core:

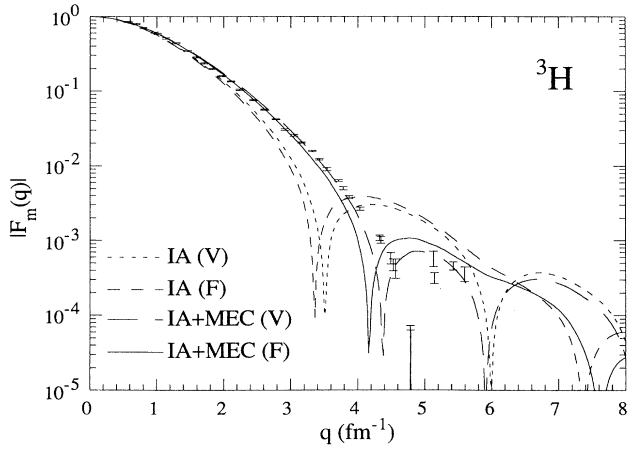

FIG. 5. Magnetic form factor $|F_m(q)|$ for ^{3}H with the Argonne v_{14}+Urbana VIII Hamiltonian calculated in impulse approximation (IA) and with meson-exchange-current (IA+MEC) contributions for both variational (V) and Faddeev (F) wave functions.

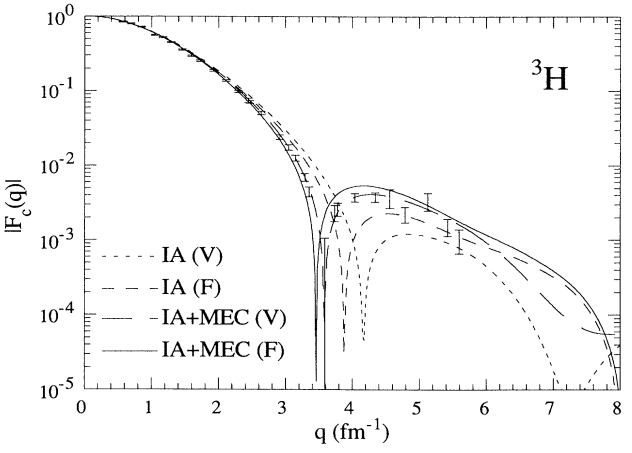

FIG. 7. Charge form factor $|F_c(q)|$ for ^{3}H with the Argonne v_{14}+Urbana VIII Hamiltonian calculated in impulse approximation (IA) and with meson-exchange-current (IA+MEC) contributions for both variational (V) and Faddeev (F) wave functions.

$$|\Psi_J\rangle = A\left\{\prod_{1\le i<j\le 4} f_{ss}(r_{ij}) \prod_{1\le k\le 4} f_{sp}(r_{5k})|\Phi_\alpha(0000)\times\Phi_p(JMTT_3)\rangle\right\} . \tag{5.1}$$

Here f_{ss} and f_{sp} are central pair-correlation functions for pairs within the s-shell, and between the s- and p-shells, respectively. The single-particle wave function for the p-shell nucleon is

$$|\Phi_p(JMTT_3)\rangle = \phi_p(R_{5\alpha})[Y_1^{m_1}(\Omega_{5\alpha})\times\chi_5(\tfrac{1}{2}m_s)]_{JM}v_5(\tfrac{1}{2}t_3) , \tag{5.2}$$

with ϕ_p a function of the coordinate $R_{i\alpha}=r_i-R_\alpha^{\rm cm}$. For ^{5}He, i.e., the n-^{4}He scattering system, we wish to study the spin-orbit splitting, which requires calculating with both $\Phi_p(\frac{3}{2}\,\frac{3}{2}\,\frac{1}{2}\,-\frac{1}{2})$ and $\Phi_p(\frac{1}{2}\,\frac{1}{2}\,\frac{1}{2}\,-\frac{1}{2})$ states. The antisymmetrization operator in Eq. (5.1) means that a sum over five terms must be taken in which each particle takes its turn in the p-shell.

For $A=6$ systems, a plausible Jastrow function puts two nucleons into p-shell orbitals with respect to an α-particle core:

$$|\Psi_J\rangle = A\left[\prod_{1\le i<j\le 4} f_{ss}(r_{ij}) \prod_{1\le k\le 4} f_{sp}(r_{5k})f_{sp}(r_{6k})f_{pp}(r_{56})|\Phi_\alpha(0000)\times\Phi_{pp}(JMTT_3)\rangle\right] . \tag{5.3}$$

Here f_{pp} is an additional central correlation between the two nucleons in the p-shell, and

$$\begin{aligned}|\Phi_{pp}(JMTT_3)\rangle = {}&\phi_p(R_{5\alpha})\phi_p(R_{6\alpha})\\ &\times\{[Y_1^{m_1}(\Omega_{5\alpha})\times Y_1^{m_1}(\Omega_{6\alpha})]_{LM_L}\\ &\times[\chi_5(\tfrac{1}{2}m_s)\times\chi_6(\tfrac{1}{2}m_s)]_{SM_S}\}_{JM}\\ &\times[v_5(\tfrac{1}{2}t_3)\times v_6(\tfrac{1}{2}t_3)]_{TT_3} .\end{aligned} \tag{5.4}$$

Now antisymmetrization means there are 15 terms to be summed over in Eq. (5.3), where each possible pair of nucleons is in the p shell. The specific Φ_{pp} of interest are $\Phi_{pp}(0\,0\,1\,-1)$ for ^{6}He, and $\Phi_{pp}(1\,1\,0\,0)$ for ^{6}Li.

The role of f_c in the Jastrow wave function of Eq. (1.6) has been split into multiple parts f_{ss}, f_{sp}, and f_{pp} in Eqs. (5.1) and (5.3). These pieces must have a similar short-range behavior, as dictated by the core of v_{ij}, but may have different long-range behaviors. For example, the asymptotic behavior of the scattered neutron in ^{5}He can be built entirely into ϕ_p, so that f_{sp} would simply go to a constant, instead of having the exponential tail of Eq. (2.6). In principle, one would also like to allow for the possible splitting of the noncentral u_p functions of Eq. (1.7) into different pieces. Unfortunately, such a split would be very expensive to compute, given the need to symmetrize the noncommuting U_{ij} operators and antisymmetrize Ψ_J.

Calculations of ^{5}He, ^{6}He, and ^{6}Li with the trial functions of Eqs. (5.1)–(5.4) are in progress; the computational effort required is reported in Table IV. The initial goal is to obtain reasonable descriptions of the spin-orbit split-

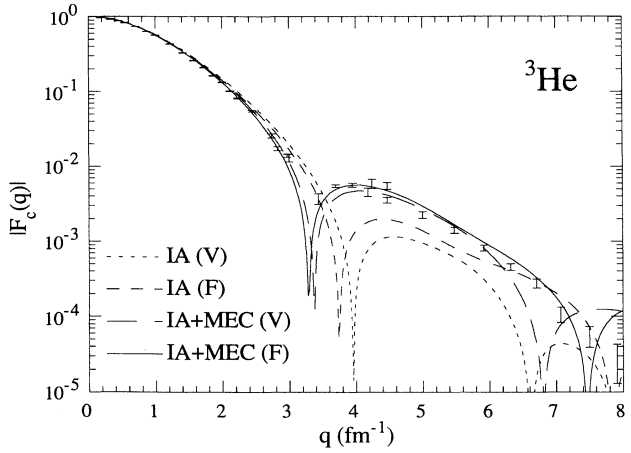

FIG. 8. Charge form factor $|F_c(q)|$ for ^{3}He with the Argonne v_{14}+Urbana VIII Hamiltonian calculated in impulse approximation (IA) and with meson-exchange-current (IA + MEC) contributions for both variational (V) and Faddeev (F) wave functions.

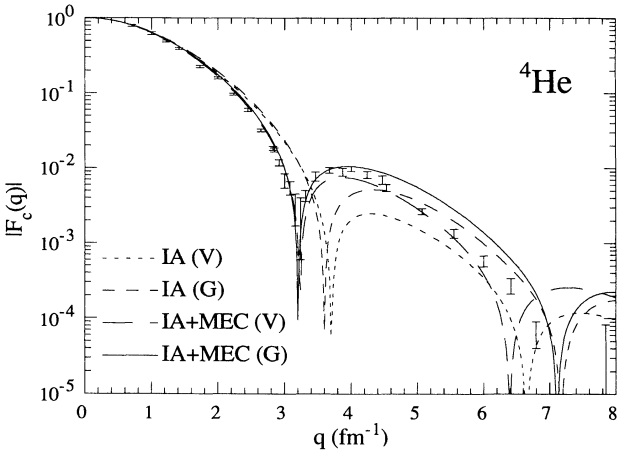

FIG. 9. Charge form factor $|F_c(q)|$ for ^{4}He with the Argonne v_{14}+Urbana VIII Hamiltonian calculated in impulse approximation (IA) and with meson-exchange-current (IA+MEC) contributions for both variational (V) and Green's function Monte Carlo (G) wave functions.

TABLE VIII. Magnetic moments for three-body nuclei, calculated in impulse approximation (IA) and with model-independent (MI) and model-dependent (MD) exchange-current contributions.

Wave function	$U_{ij}+U_{ij}^{LS}+U_{ijk}^{\mathrm{TNI}}$ isoscalar	Faddeev	$U_{ij}+U_{ij}^{LS}+U_{ijk}^{\mathrm{TNI}}$ isovector	Faddeev
IA	0.404	0.403	−2.182	−2.168
IA+MI	0.422	0.420	−2.561	−2.535
IA+MI+MD	0.428	0.427	−2.630	−2.602
Experiment	0.426		−2.553	
	^{3}H		^{3}He	
IA	2.586	2.571	−1.778	−1.765
IA+MI	2.983	2.955	−2.139	−2.115
IA+MI+MD	3.058	3.029	−2.202	−2.175
Experiment	2.979		−2.127	

ting in ^{5}He, and the binding energies of ^{6}He and ^{6}Li. Earlier variational Monte Carlo calculations of ^{5}He with a trial function of the U_{ij} form gave about 60% of the spin-orbit splitting.[23] Previous calculations of six-body nuclei as six-body problems have been limited to simple central force models.[24] (As a test of our six-body code we have reproduced the variational results of Ref. 24).

The six-body nuclei are weakly bound systems: ^{6}He at 29.3 MeV is bound by only 1 MeV relative to a separated α and two neutrons, while ^{6}Li at 32.0 MeV is bound by only 1.5 MeV relative to a separated α and a deuteron. Current results suggest that obtaining six-body nuclei stable against particle breakup with realistic interaction models is nontrivial. For example, with the Argonne v_{14} plus Urbana VII model, a variational wave function of the form described above that has the correct charge radius for ^{6}Li gives a binding energy of 30.8±0.3 MeV. While this is not so far from the experimental binding energy, it is well above the variational upper bound for a separated α and deuteron of 32.7 MeV for this Hamiltonian.

Possible explanations for this difficulty are that the variational ansatz described above is not adequate, or that the variational parameter space has not yet been explored adequately. It is also possible the the Hamiltonian is at fault. Recent studies of ^{16}O with the same model using comparable variational wave functions in a cluster expansion Monte Carlo calculation[9] give only 0.3 MeV/nucleon more binding for ^{16}O than for ^{4}He, compared to an experimental difference of 0.9 MeV/nucleon. It may be that ^{6}He and ^{6}Li are simply not stable with this Hamiltonian. The very crude form for the short-range part of the three-nucleon interaction is the most likely culprit in this case. Calculations of p-shell nucleon could provide key information for making better models of the three-nucleon interaction.

VI. CONCLUSIONS

In summary, we have reported a set of improvements for variational trial functions in few-body nuclei. We have shown that they give upper bounds to the binding energy that are typically 3–4% above available exact calculations in ^{3}H and ^{4}He. The extension to a six-operator correlation, U_{ij}, is a straightforward and inexpensive step. The addition of a three-nucleon interaction correlation, U_{ijk}^{TNI}, makes a significant improvement when a three-body potential, V_{ijk}, is present in the Hamiltonian, which completely justifies the extra cost of its computation. The addition of a spin-orbit correlation U_{ij}^{LS} gives only a very marginal improvement by itself, which may not justify its expense. However, it seems to be more important in the presence of V_{ijk} and U_{ijk}^{TNI} and it may be expected to play a more significant role in p-shell nuclei. We have also discussed how these wave functions may be extended for the five- and six-body nuclei.

Obtaining a consistent description of nuclear systems, from few-body nuclei to nuclear matter, with realistic interactions using nonrelativistic quantum mechanics, is a challenging problem. The solution will require continuing advances in both the many-body theory and the Hamiltonian, particularly in the many-nucleon part of the interaction.

ACKNOWLEDGMENTS

I wish to thank my colleagues J. Carlson, V. R. Pandharipande, S. C. Pieper, D. Riska, and R. Schiavilla for their continuing comments and advice. I also wish to thank C. R. Chen, J. L. Friar, B. F. Gibson, and G. L. Payne for the use of their Faddeev wave functions. The calculations reported here were made possibly by grants of time on the Cray computers at the National Energy Research Computation Center, Livermore, and the National Center for Supercomputing Applications, Urbana, Ill. This work is supported by the U.S. Department of Energy, Nuclear Physics Division, under Contract No. W-31-109-ENG-38.

[1]R. V. Reid, Ann. Phys. (N.Y.) **50**, 411 (1968); R. B. Wiringa and V. R. Pandharipande, Nucl. Phys. **A317**, 1 (1979).
[2]R. B. Wiringa, R. A. Smith, and T. L. Ainsworth, Phys. Rev. C **29**, 1207 (1984).
[3]M. Lacombe, B. Loiseau, J. M. Richard, R. Vinh Mau, J. Côte, P. Pireś, and R. de Tourreil, Phys. Rev. C **21**, 861 (1980).
[4]J. Fujita and H. Miyazawa, Prog. Theor. Phys. **17**, 360 (1957).
[5]S. A. Coon, M. D. Scadron, P. C. McNamee, B. R. Barrett, D. W. E. Blatt, and B. H. J. McKellar, Nucl. Phys. **A317**, 242 (1979).
[6]J. Carlson, V. R. Pandharipande, and R. B. Wiringa, Nucl. Phys. **A401**, 59 (1983).
[7]R. Schiavilla, V. R. Pandharipande, and R. B. Wiringa, Nucl. Phys. **A449**, 219 (1986).
[8]J. Lomnitz-Adler, V. R. Pandharipande, and R. A. Smith, Nucl. Phys. **A361**, 399 (1981).
[9]S. C. Pieper, R. B. Wiringa, and V. R. Pandharipande, Phys. Rev. Lett. **64**, 364 (1990).
[10]V. R. Pandharipande and R. B. Wiringa, Rev. Mod. Phys. **51**, 821 (1979).
[11]I. E. Lagaris and V. R. Pandharipande, Nucl. Phys. **A359**, 349 (1981).
[12]R. B. Wiringa, V. Fiks, and A. Fabrocini, Phys. Rev. C **38**, 1010 (1988).
[13]R. Schiavilla, V. R. Pandharipande, and D. O. Riska, Phys. Rev. C **40**, 2294 (1989); **41**, 309 (1990).
[14]R. Schiavilla and D. O. Riska, Phys. Lett. B **244**, 373 (1990).
[15]J. Lomnitz-Adler and V. R. Pandharipande, Nucl. Phys. **A342**, 404 (1980).
[16]N. Metropolis, A. W. Rosenbluth, M. N. Rosenbluth, A. H. Teller, and E. Teller, J. Chem. Phys. **21**, 1087 (1953).
[17]C. R. Chen, G. L. Payne, J. L. Friar, and B. F. Gibson, Phys. Rev. C **31**, 2266 (1985); **33**, 1740 (1986); private communication.
[18]J. Carlson, Phys. Rev. C **38**, 1879 (1988); Los Alamos Report No. LA-UR-90-2088, 1990.
[19]J. Carlson and R. B. Wiringa, in *Computational Nuclear Physics,* edited by S. E. Koonin, K. Langanke, J. A. Maruhn, and M. R. Zirnbauer (Springer-Verlag, Berlin, 1991).
[20]R. B. Wiringa, Nucl. Phys. **A401**, 86 (1983).
[21]R. B. Wiringa, C. R. Chen, G. L. Payne, J. L. Friar, and B. F. Gibson, Phys. Lett. **143B**, 273 (1984).
[22]G. Höhler *et al.*, Nucl. Phys. B **114**, 505 (1976).
[23]J. Carlson, K. E. Schmidt, and M. H. Kalos, Phys. Rev. C **36**, 27 (1987).
[24]Y. Alhassid, G. Maddison, K. Langanke, K. Chow, and S. E. Koonin, Z. Phys. A **321**, 677 (1984).